

Hyperglycemia-Induced Vasculopathy in the Murine Vitelline Vasculature

Correlation with PECAM-1/CD31 Tyrosine Phosphorylation State

Emese Pinter,^{*†} Sepi Mahooti,^{*} Yi Wang,[‡]
Beat A. Imhof,[§] and Joseph A. Madri^{*}

From the Departments of Pathology^{*} and Pediatrics,[†] Yale University, and Alexion Pharmaceuticals, Inc.,[‡] New Haven, Connecticut, and the Department of Pathology,[§] University of Geneva, Geneva, Switzerland

Maternal diabetes mellitus is associated with an increased incidence of congenital abnormalities as well as embryonic and perinatal lethality. In particular, a wide range of cardiovascular abnormalities have been noted in children of diabetic mothers and in the offspring of diabetic animals. The vascular system is the first organ system to develop in the embryo and is critical for normal organogenesis. The organization of mesodermal cells into endothelial and hematopoietic cells and into a complex vascular system is, in part, mediated by a series of specific cell-cell, cell-extracellular matrix, and cell-factor interactions. PECAM-1 expression has been observed during the earliest stages of vasculogenesis, and changes in PECAM-1 tyrosine phosphorylation have been associated with endothelial cell migration, vasculogenesis, and angiogenesis both *in vitro* and *in vivo*. In this report we demonstrate that exposure to hyperglycemia during gastrulation causes yolk sac and embryonic vasculopathy in cultured murine conceptuses and in the conceptuses of streptozotocin-induced diabetic pregnant mice. In addition, we correlate the presence of yolk sac and embryonic vasculopathy with the failure of PECAM-1 tyrosine dephosphorylation during the formation of blood islands/vessels from clusters of extra-embryonic and embryonic angioblasts in the murine conceptus using both *in vitro* and *in vivo* models. The importance of these findings in the development of vasculopathy in the offspring of diabetic mothers and the potential effects and benefits of glucose regulation during the periods of vasculogenesis/angiogenesis in embryonic development are discussed. (Am J Pathol 1999, 154:1367-1379)

It is well known that maternal diabetes mellitus is a predisposition for embryonic lethality and congenital abnormalities.¹⁻⁸ Meticulous metabolic control of maternal diabetes mellitus has significantly decreased the risk of gross structural malformations; nevertheless, the incidence of these abnormalities is still three to five times higher than that among nondiabetic women. A wide range of observed congenital abnormalities have been noted in the offspring of diabetic mothers. Although no particular or specific abnormalities have been associated with maternal diabetes, abnormalities of the cardiovascular system occur frequently.⁴ Experimentally induced diabetes in animals and hyperglycemia in a rodent conceptus culture system resulted in similar abnormalities as observed in humans.^{7,8}

Recently, there have been significant advances in our understanding of vasculogenesis and angiogenesis that illustrate the complex interrelationships of angiogenic, survival, and differentiation factors and their receptors with cell adhesion and cell matrix adhesion molecules. Targeted disruptions of several genes have demonstrated that a series of interdependent developmental steps are necessary for the complete development and proper functioning of the circulatory system, which is necessary for normal embryonic development.⁹⁻²⁷ Furthermore, these results also demonstrate that many of the lethal abnormalities have in common the failure of the development of gestation-dependent routes of nutritional interactions between the mother and the embryo/fetus, including implantation, formation of yolk sac (vitelline) circulation, and formation of the chorioallantoic placenta.⁹⁻²⁷

One particular cell adhesion molecule, PECAM-1/CD31 (a 130-kd member of the Ig superfamily), has been found not only to be a marker of endothelial cells but also to be a modulator of endothelial cell migration, cell-cell adhesion, and *in vitro* and *in vivo* angiogenesis.²⁸⁻³³

Supported in part by USPHS grants RO1-HL-28373 and PO1-KD-38979 to J.A. Madri and RO1-HL-28373-14SL and P30-HD-27757 to E. Pinter.

Accepted for publication January 23, 1999.

Address reprint requests to Dr. J. A. Madri, Department of Pathology, Yale University School of Medicine, 310 Cedar Street, New Haven, CT 06510. E-mail: joseph.madri@yale.edu.

PECAM-1 exhibits dynamic tyrosine dephosphorylation-rephosphorylation during *in vitro* endothelial cell migration and during *in vivo* vasculogenesis.^{29,30,34} PECAM-1 tyrosine phosphorylation has been found to occur on two tyrosine residues, Y₆₆₃ and Y₆₈₆, residing in an ITAM domain.^{29,30,34} Phosphorylation of these tyrosine residues mediates binding of c-src and the phosphatase SHP-2, which have been implicated in mediating a variety of signaling events.^{29,31,34} Site-directed mutagenesis of either of these tyrosine residues with phenylalanine results in a loss of PECAM-1 tyrosine phosphorylation at both Y₆₆₃ and Y₆₈₆ and loss of src-SH2 domain and SHP-2 binding.²⁹⁻³¹ In addition, the Y₆₈₆ to F mutation results in loss of lateral border localization of PECAM-1 and abrogates PECAM-1's effect on cellular migration.^{29,34}

In this report we establish a correlation between a failure of PECAM-1 tyrosine dephosphorylation and hyperglycemia-induced yolk sac vasculopathy observed in whole embryo cultures and an animal model of streptozotocin-induced maternal diabetes. The implications of these findings with respect to the congenital abnormalities observed in maternal diabetes and PECAM-1's roles in modulating vasculogenesis and angiogenesis are discussed.

Materials and Methods

Antibodies

An affinity-purified rabbit polyclonal anti-murine PECAM-1 produced as described^{32,35} was used to immunoprecipitate PECAM-1 from yolk sac and embryo lysates.²⁹ A monoclonal anti-phosphotyrosine antibody (4G10, Upstate Biotechnology, Lake Placid, NY) was used to detect phosphotyrosine in a Western blot assay.^{29,32}

Murine Conceptuses

In mice, the period from day 7.5 postconceptual (p.c.) to 9.5 p.c. represents the time of organogenesis and the time of the development of the vitelline vasculature. Conceptuses were obtained from timed pregnant mice (CD1; Charles River, Wilmington, MA) maintained and bred under standard (12-hour daily illumination) laboratory conditions according to established, approved Yale University Animal Care Committee protocols. Mating was detected by the presence of a vaginal plug. The plug-positive day was designated p.c. day 0.5.

Harvesting of Conceptuses

At days 7.5, 8.5, and 9.5 p.c. at 10 a.m. pregnant females were sacrificed by cervical dislocation, and the conceptuses were removed from their uteri as described^{7,32} and used for morphological and biochemical studies directly or after defined periods of culture.

In Vitro Conceptus Culture

At day 7.5 p.c. at 10 a.m., pregnant females were sacrificed by cervical dislocation, and conceptuses were removed from their implantation sites as described^{7,32} and placed in Dulbecco's modified Eagle's medium (glucose content, 1 g/L; Gibco BRL, Life Technologies, Gaithersburg, MD) and separated into primitive streak, neural plate, and headfold stages according to the morphological criteria described by Downs and Davies³⁶ for subsequent culture. Reichert's membrane was removed, and primitive streak, neural plate, and early and late headfold stage conceptuses were subjected to culture as described.³²

Conceptuses were cultured (five conceptuses/60 cc Wheaton borosilicate glass serum bottle (223746, Wheaton, Millville, NJ)) in a roller bottle incubator at 30 revolutions/minute (Robbins Scientific model 1000, Sunnyvale, CA) for 24 or 48 hours in 5 ml of pooled normal male rat serum (5 mmol/L D-glucose) harvested from 300-g adult male rats, containing penicillin and streptomycin, filtered through a 0.45- μ m Millipore filter and used without dilution. Cultures were oxygenated using a series of gas mixtures having increasing oxygen concentrations (5% O₂, 5% CO₂, 90% N (0 to 24 hours), 20% O₂, 5% CO₂, 75% N (24 to 36 hours); and 40% O₂, 5% CO₂, 55% N (36 to 48 hours)) as described previously.^{2,7,32,37}

Groups of 25 control embryos cultured in male rat serum and experimental embryos cultured in male rat serum supplemented with 15 mmol/L of either α L-glucose, D-mannitol or α D-glucose (Sigma Chemical Co., St. Louis, MO) were used in the morphological and biochemical studies. The osmolality of the control sera was determined to be 280 mOsm/kg, and the osmolality of the hyperglycemic sera was found to be 305 mOsm/kg, both well below the 370 to 380 mOsm/kg range previously reported to be teratogenic.²

Aortas of adult (6- to 8-week-old) mice were harvested and used as a source of quiescent endothelial cells (controls) in biochemical studies.

In another series of experiments, primitive streak and early headfold conceptuses were cultured for 3 hours in the above described hyperglycemic sera and then transferred and cultured in normal sera for an additional 45 hours. Yolk sacs and embryos were separated at the end of the 48-hour culture period, and the specimens were assessed for the presence or absence of major structural/functional defects (presence of heart beat, yolk sac circulation, neural tube closure, and completion of axial rotation), and growth and development were scored by the organ primordia development criteria outlined by Kaufman.³⁹ The yolk sacs and embryos were then subjected to biochemical and morphological studies as described previously.³²

Streptozotocin Treatment

Six- to eight-week-old virgin, female mice (CD1, Charles River, Wilmington, MA) were injected under Metaphane

anesthesia with 250 mg/kg streptozotocin (Sigma) freshly dissolved in 5 mmol/L citrate buffer, pH 4.5, into the tail vein before mating. Control animals received an equivalent volume of buffered citrate solution.^{2,3} Animals were screened for the onset of diabetes every other day by measuring urine glucose levels (Chemstrip, Boehringer Mannheim, Indianapolis, IN). Onset of diabetes was determined as a urine glucose level greater than 250 mg/dl (25 mmol/L) for two consecutive readings and a blood glucose level greater than 200 mg/dl (20 mmol/L). The majority of streptozotocin-treated mice became diabetic within 2 weeks. Diabetic mice received daily injections of 1 to 2 U of human recombinant insulin before and 1 day after mating. The mean glucose level of normal mothers was 5 mmol/L. The diabetic mothers' glucose levels were 20 to 25 mmol/L. Matings were performed as described above. Conceptuses harvested from control and streptozotocin-treated nondiabetic and diabetic mothers were collected at day 9.5 p.c. and subjected to morphological and biochemical analyses.

Whole-Mount Immunostaining of Conceptuses

Conceptuses were rinsed in 100 mmol/L phosphate buffer (PB), pH 7.4, before fixation in 4% freshly prepared paraformaldehyde in PB for 2 hours at 4°C. Specimens were then dehydrated in methanol and kept in 100% methanol at -20°C until use.

Immunostaining was performed using the avidin-biotin complex technique (ABC kit; Vector Laboratories, Burlingame, CA) according to the manufacturer's instructions. Briefly, after permeabilization with 0.04% Triton X-100 in PB for 1 hour at 4°C, the yolk sacs were incubated with a 1:1000 dilution (1 µg/ml) of anti-PECAM-1 antibody overnight at 4°C. After three washes with PB, the yolk sacs and embryos were incubated with avidin-peroxidase for 1 hour, washed, and incubated with a solution of 15 mg of diaminobenzidine, 12 mg of ammonium chloride, and 0.12 mg of glucose oxidase in 30 ml of PB and 600 µl of a solution of nickel-ammonium sulfate 0.05 mol/L in sodium acetate buffer, pH 6.0, for 5 minutes. Normal rabbit IgG was used in place of the primary antibody in controls. At day 9.5 p.c. and at the end of the 48-hour culture period, 20 to 25 randomly selected conceptuses were stained and evaluated for vessel development.

In addition, several yolk sacs were placed in a fixative containing 1.5% paraformaldehyde and 1.5% glutaraldehyde in 0.1 mmol/L PB at pH 7.4. After overnight fixation, the yolk sacs were washed in several changes of PB. After post-fixation with osmium (0.5% OsO₄) for 10 minutes, the yolk sacs were dehydrated and embedded in Araldite. Semi-thin and ultrathin sections were examined using light and electron microscopy (Zeiss EM910), respectively, as described.³⁸

Immunoprecipitation and Western Blotting

Conceptuses from several litters were separated into developmental stages as described and pooled to obtain enough starting material to attain 200-µg protein aliquots

for immunoprecipitations. Primitive streak, neural plate, and early headfold stage day 7.5 p.c. conceptuses and yolk sacs of *in vivo*-grown conceptuses from normoglycemic and hyperglycemic mothers and yolk sacs of cultured conceptuses (normal and hyperglycemic conditions) at day 9.5 p.c. were placed in ice-cold lysis buffer (50 mmol/L Tris HCl, pH 7.4, 0.5% Triton X-100, 0.05% deoxycholate, 0.5 mmol/L sodium orthovanadate, and protease inhibitor cocktail (complete protease inhibitor, Boehringer Mannheim). The lysates were centrifuged at 14,000 × *g* at 4°C for 10 minutes, and the supernatants were assayed for protein concentration (Pierce). PECAM-1 was immunoprecipitated from 200-µg aliquots of lysates of conceptuses and yolk sacs with 5 µg of polyclonal anti-PECAM-1 antibody as described.³² Immunoprecipitates were separated by SDS-PAGE under reducing conditions and electroblotted onto Immobilon P membranes (Millipore Corp., Bedford, MA). Western blot analyses were performed as described^{29,32} using anti-phosphotyrosine antibody (4G10) at 1:1000 dilution³² followed by horseradish-peroxidase-conjugated goat anti-mouse antibody (Promega, Madison, WI) at a dilution of 1:15,000. Antibody binding was detected using the enhanced chemiluminescence detection system (Amersham Corp., Arlington Heights, IL) according to the manufacturer's instructions. The blots were then stripped and reprobed with polyclonal anti-PECAM-1 antibody at a dilution of 1:2000 followed by horseradish-peroxidase-conjugated goat anti-rabbit antibody (Promega, Madison, WI) at a dilution of 1:20,000, and detection was performed as before. Experiments were performed three to five times on five different sets of harvested and cultured conceptuses and yolk sacs. All blots were scanned into a Power Macintosh 9600 computer using an Arcus II scanner and Photoshop 4.0 software. Quantitation of bands was performed using BioMax software (Kodak, Rochester, NY). Statistics were performed using Microsoft Excel software (Microsoft, Bothell, WA). Photomicrographs were produced using an Epson stylus 800 color printer.

Results

Primitive Streak and Neural Plate Stage Conceptus Cultures Made Hyperglycemic Exhibit Yolk Sac Vasculopathy

Murine conceptuses harvested at day 7.5 p.c. and cultured for 48 hours as described^{7,32} undergo normal organogenesis, including the development of the first interconnecting circulatory system between a vascularized extra-embryonic membrane (the yolk sac) and the developing embryo: the vitelline circulation.^{7,39} In previous studies we have reported that exposure of cultured rodent conceptuses to serum containing excess D-glucose resulted in retarded and anomalous embryonic development and differentiation when compared with *in vivo* controls cultured under identical conditions without added D-glucose.⁷

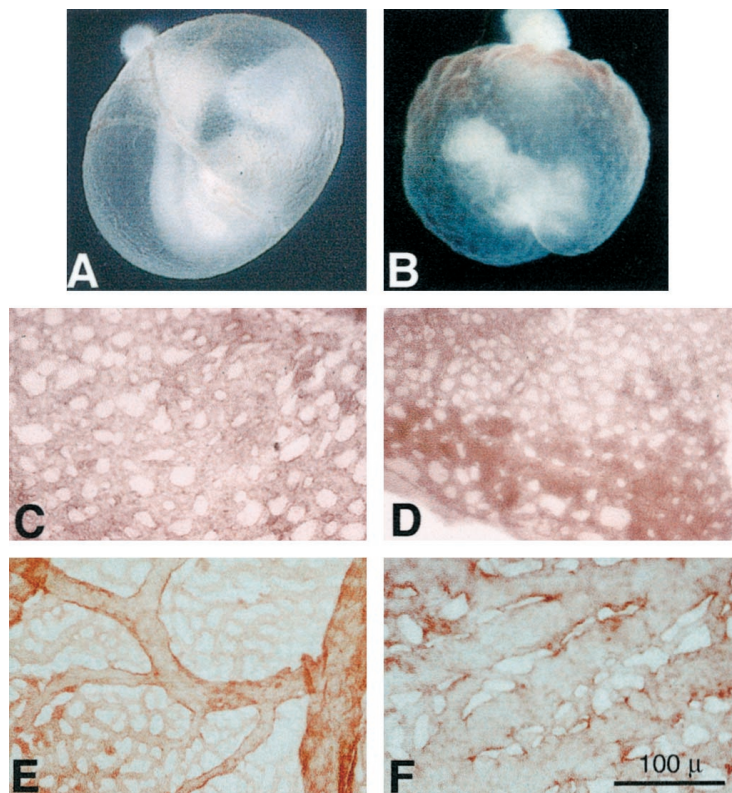


Figure 1. **A** and **B:** Morphological analyses (whole mount) of the developing yolk sac vasculature at day 9.5 p.c. in conceptuses harvested from normoglycemic mothers and cultured in normoglycemic (5 mmol/L D-glucose) (**A**) or in hyperglycemic conditions (20 mmol/L D-glucose) (**B**). **A:** Representative conceptus harvested at 7.5 day p.c. from a normoglycemic mother and cultured for 48 hours in normoglycemic media, illustrating the normal delicate arborization of the yolk sac vasculature. **B:** Representative conceptus harvested at 7.5 day p.c. from a normoglycemic mother and cultured for 48 hours in hyperglycemic media, illustrating the arrest of yolk sac vasculo- and angiogenesis at the primary capillary plexus stage, depicted by ectatic vascular channels with no apparent arborization. **C** to **F:** Morphological analyses of the developing yolk sac vasculature at days 8.5 and 9.5 p.c. in normoglycemic (**C** and **E**) and hyperglycemic (**D** and **F**) culture conditions. **C:** Low-power *en face* representative micrograph of the yolk sac primary capillary plexus observed in a conceptus harvested at day 7.5 p.c. and cultured for 24 hours (now a day 8.5 p.c. conceptus) in normoglycemic conditions labeled with anti-PECAM-1. Note the network of branching channels of fairly uniform diameter. Scale bar, 100 μ m. **D:** Low-power *en face* representative micrograph of the yolk sac primary capillary plexus observed in a conceptus harvested at day 7.5 p.c. and cultured for 24 hours (now a day 8.5 p.c. conceptus) in hyperglycemic conditions labeled with anti-PECAM-1. Note the network of branching channels of fairly uniform diameter similar to that illustrated in **C**. **E:** Low-power *en face* representative micrograph of the yolk sac vasculature observed in a conceptus harvested at day 7.5 p.c. and cultured for 48 hours (now a day 9.5 p.c. conceptus) in normoglycemic conditions labeled with anti-PECAM-1. Note the arborizing network of vessels composed of branching vessels of decreasing diameters as they branch from the larger vessels. **F:** Low-power *en face* representative micrograph of the yolk sac vasculature observed in a conceptus harvested at day 7.5 p.c. and cultured for 48 hours (now a day 9.5 p.c. conceptus) in hyperglycemic conditions labeled with anti-PECAM-1. Note the network of branching channels composed of ectatic vessel segments with occasional smaller branches having larger diameters than the terminal branching vessels observed in **E**. Scale bar, 100 μ m. Experiments were performed at least five times with separate litters.

To determine the effects of hyperglycemia on vasculogenesis, conceptuses were cultured in the presence of 50, 20, or 12 mmol/L D-glucose for 48 hours (glucose level in control sera was 5 mmol/L). All elevated D-glucose concentrations tested were observed to induce yolk sac vasculopathy. As no major differences in yolk sac vascular abnormalities were noted among these glucose concentrations, all additional experiments were carried out using 20 mmol/L D-glucose. As illustrated in Figure 1, normal yolk sac and vitelline vascular development (including arborization) is observed in the conceptuses cultured in normoglycemic conditions (5 mmol/L glucose; Figure 1A), whereas a profoundly abnormal yolk sac and vitelline vasculature is noted in the conceptuses cultured in hyperglycemic conditions (20 mmol/L D-glucose; Figure 1B). Yolk sacs were dissected away from the embryos and stained using anti-PECAM-1 and examined as whole-mount specimens. These findings prompted further investigations of the yolk sac vasculature. PECAM-1

localization was detected using a secondary antibody coupled to a biotin-avidin-peroxidase complex and subsequent development of the diaminobenzidine reaction product, illustrating the yolk sac vasculature. At day 8.5, a primary capillary plexus had developed in the control yolk sacs (Figure 1C), which further develops into an arborizing interconnecting vascular network composed of arteries, veins, and capillaries exhibiting blood flow by day 9.5 (Figure 1E). Umbilical arteries and veins were attached to the chorionic plate.

In contrast, in the presence of 20 mmol/L D-glucose, the yolk sac vasculature does not develop past the primary capillary plexus stage noted at day 8.5 (Figure 1D) but appears arrested as a branching ectatic plexus with no apparent arborization or distinction of arteries and veins (Figure 1F). These findings are similar to the arrest of vascular development noted in the embryonic lethal tissue factor null conceptuses in which the yolk sac vasculature was arrested in the primary capillary plexus

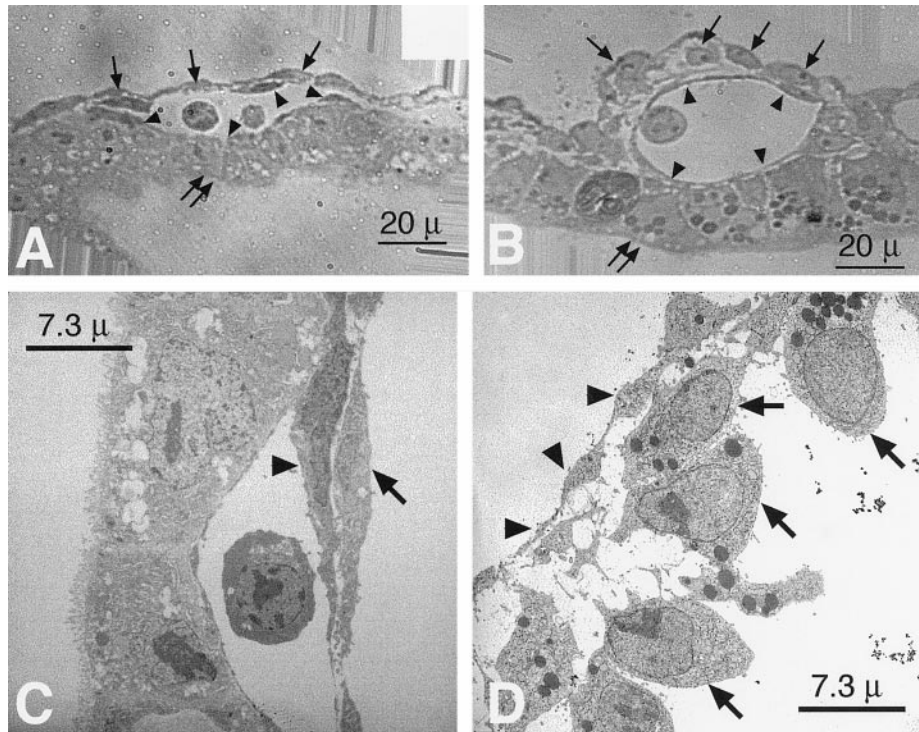


Figure 2. Light (A and B) and electron microscopic (C and D) analyses of the developing yolk sac vasculature at day 9.5 p.c. in normoglycemic (A and C) and hyperglycemic (B and D) culture conditions. **A:** High-power representative light micrograph of the terminal yolk sac vasculature capillaries observed in a conceptus harvested at day 7.5 p.c. and cultured for 48 hours (now a day 9.5 p.c. conceptus) in normoglycemic conditions. Note the vessel lined by flattened endothelial cells (arrowheads) containing two circulating blood cells in the lumen, bordered by the endodermal cells on one aspect (double arrows) and flattened, elongated mesenchymal cells (pericytes) and mesothelial cells on the other aspect (arrows) in close contact with the abluminal surfaces of the endothelium. Scale bar, 20 μm . **B:** High-power representative light micrograph of the terminal yolk sac vasculature capillaries observed in a conceptus harvested at day 7.5 p.c. and cultured for 48 hours (now a day 9.5 p.c. conceptus) in hyperglycemic conditions. Note the vessel lined by flattened endothelial cells (arrowheads), bordered by the endodermal cells on one aspect (double arrows) and plump, rounded, mesenchymal cells (pericytes) and mesothelial cells on the other aspect (arrows) in loose contact with the abluminal surfaces of the endothelium. A blood cell is noted in the lumen. Scale bar, 20 μm . **C:** Representative transmission electron micrograph of the terminal yolk sac vasculature capillaries observed in a conceptus harvested at day 7.5 p.c. and cultured for 48 hours (now a day 9.5 p.c. conceptus) in normoglycemic conditions. Note the vessel lined by flattened endothelial cells (arrowheads) bordering the lumen and the flattened, elongated mesenchymal cells (pericytes) in close contact with the abluminal surfaces of the endothelium. A blood cell is noted in the lumen. Scale bar, 7.3 μm . **D:** Representative transmission electron micrograph of the terminal yolk sac vasculature capillaries observed in a conceptus harvested at day 7.5 p.c. and cultured for 48 hours (now a day 9.5 p.c. conceptus) in hyperglycemic conditions. Note the vessel lined by flattened endothelial cells (arrowheads) bordering the lumen and the plump, rounded, mesenchymal cells (pericytes) in loose contact with the abluminal surfaces of the endothelium. Scale bar, 7.3 μm . Experiments were performed at least five times with separate litters.

stage and appeared as ectatic capillary segments. Additionally, despite the presence of an embryonic heart beat, no circulation was observed in these conceptuses. Additional light and electron microscopic examination of the yolk sac vasculature at day 9.5 p.c. confirmed the initial observations. Cross sections of yolk sac capillaries from control conceptuses revealed small-diameter vessels lined by flattened, elongated endothelial cells containing occasional circulating blood cells and tightly invested by elongated, flattened mesenchymal and mesodermal cells (Figure 2, A and C). In contrast, cross sections of yolk sac capillaries from 20 mmol/L D-glucose-treated conceptuses revealed larger-diameter, ectatic capillaries filled with blood cells, demarcated by flattened endothelial cells and loosely invested with plump, rounded mesenchymal and mesodermal cells (Figure 2, B and D). Conceptuses cultured with media containing added L-glucose or D-mannitol were observed to develop normally, with no detectable abnormalities (see Table 1).

Tyrosine Phosphorylation of PECAM-1 is Modulated by D-Glucose Levels in Cultured Conceptuses

We previously demonstrated the presence of PECAM-1 in early undifferentiated angioblasts at day 7.5 p.c. and in endothelial cells lining vessels of the developing vascular system at day 9.5 p.c.³² We have also reported a decrease in PECAM-1 tyrosine phosphorylation during vasculogenesis from day 7.5 p.c. to day 9.5 p.c.³² To assess possible correlations between the arrest of yolk sac vasculogenesis and PECAM-1 tyrosine phosphorylation we performed immunoprecipitations followed by Western blot analyses. Lysates from conceptuses at day 7.5 and lysates of yolk sacs at day 9.5 p.c. cultured in pooled rat serum and pooled rat serum supplemented to 20 mmol/L D-glucose were immunoprecipitated with polyclonal anti-PECAM-1. After SDS-PAGE of the precipitates and electroblotting, the blots were analyzed using antibodies di-

Table 1. Hyperglycemia-Induced Yolk Sac Vasculopathy Is Developmental Stage-Dependent

| Developmental stages at 7.5 days p.c. | Yolk sac vasculopathy |
|---|-----------------------|
| (20 mmol/L D-glucose) Primitive streak stages 50% | 25/25 (100%) |
| (20 mmol/L D-glucose) Neural plate stages 38% | 22/22 (100%) |
| (20 mmol/L D-glucose) Headfold stages 12% | 03/32 (9%) |
| (15 mmol/L L-glucose) (5 mmol/L D-glucose) Primitive streak stages Neural plate stages | 06/86 (7%) |
| (15 mmol/L D-mannitol)(5 mmol/L D-glucose) Primitive streak stages Neural plate stages | 02/35 (6%) |
| Normoglycemic (5 mmol/L D-glucose) Control cultures | 04/189 (2%) |

The incidence of yolk sac vasculopathy (arrest of the vasculature at the primary capillary plexus stage) was determined in stage-sorted day 7.5 p.c. conceptuses harvested from several mothers. As illustrated, conceptuses at the primitive streak and neural plate stages exhibited 100% yolk sac vasculopathy, whereas only 9% of conceptuses at headfold stages exhibited any yolk sac vasculopathy when cultured in hyperglycemic conditions (20 mmol/L D-glucose). Conceptuses cultured in rat sera supplemented with either 15 mmol/L α-glucose or 15 mmol/L D-mannitol exhibited incidences of 7% and 6% vasculopathy, respectively. Day 7.5 p.c. conceptuses cultured in normoglycemic conditions (5 mmol/L D-glucose) exhibited a 2% incidence of vasculopathy.

rected against phosphotyrosine (PY) and PECAM-1 (Figure 3). These data demonstrate the presence of PECAM-1 at both time points by immunoprecipitation followed by Western blotting with PECAM-1 antibodies

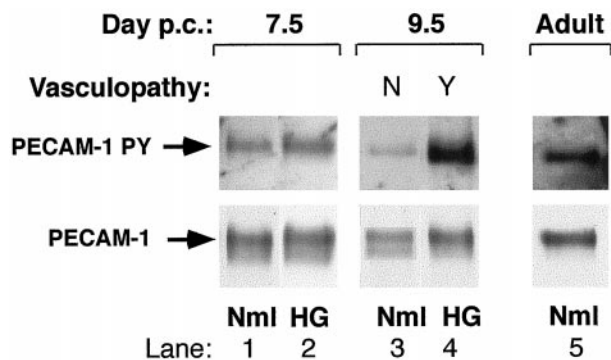


Figure 3. Representative immunoprecipitation/Western blot analyses of PECAM-1 expression and tyrosine phosphorylation of yolk sacs isolated from day 7.5 and 9.5 p.c. conceptuses cultured in normoglycemic (Nml) and hyperglycemic (HG) conditions. Note the similar expression levels of PECAM-1 at day 7.5 and 9.5 p.c. in all conditions when the yolk sac lysates were immunoprecipitated with anti-PECAM-1 and then blotted using anti-PECAM-1 (lower panel). Stripping and reprobing these blots with anti-phosphotyrosine revealed relatively high tyrosine phosphorylation of PECAM-1 at day 7.5 p.c. in both normo- and hyperglycemic conditions (lanes 1 and 2, upper panel). However, at day 9.5 p.c. the normoglycemic yolk sac PECAM-1 was observed to exhibit a reduced tyrosine phosphorylation compared with the day 7.5 p.c. lysates, (0.38 versus 1.00 when quantitated, normalized to PECAM-1 expression and compared; lane 3, upper panel). In contrast, the day 9.5 p.c. hyperglycemic yolk sac PECAM-1 exhibited an increased tyrosine phosphorylation compared with the day 7.5 p.c. lysates and the day 9.5 p.c. normoglycemic lysate (2.53 versus 1.00 and 0.38) when quantitated, normalized to PECAM-1 expression and compared (lane 4, upper panel). Adult (6 weeks of age) aortic endothelial cell lysates were used as representative quiescent endothelial cells and assayed for comparison (lane 5). Experiments were performed at least five times with separate litters, all yielding similar results (see Figure 7 for quantitation).

(lower panel). Additionally, blotting the PECAM-1 immunoprecipitates with anti-phosphotyrosine³² revealed that PECAM-1 isolated from the day 7.5 p.c. yolk sacs was highly tyrosine phosphorylated compared with PECAM-1 isolated from the day 9.5 p.c. yolk sacs cultured in pooled rat serum (compare lanes 1 and 3 of Figure 3 and see Figure 7, 1.00 ± 0.1 versus 0.38 ± 0.1, n = 3, P < 0.05). In contrast, when PECAM-1 isolated from the day 9.5 p.c. yolk sacs cultured in pooled rat serum supplemented to a final concentration of 20 mmol/L D-glucose was immunoprecipitated and blotted with anti-phosphotyrosine reagents, the PECAM-1 exhibited a high tyrosine phosphorylation state compared with PECAM-1 isolated from the day 9.5 p.c. yolk sacs cultured in pooled rat serum (compare lanes 3 and 4 of Figure 3 and see Figure 7, 2.53 ± 0.99 versus 0.38 ± 0.1, n = 3, P < 0.05). Resting adult endothelial cells (harvested from adult mouse aortas) exhibit a PECAM-1 tyrosine phosphorylation level similar to that observed in the 7.5 day p.c. conceptuses, as would be expected in resting endothelium (lane 5 of Figure 3).²⁹ PECAM-1 tyrosine phosphorylation states in conceptuses cultured with media containing added L-glucose or D-mannitol showed PECAM-1 phosphorylation states indistinguishable from those noted in control cultures and from conceptuses harvested from control mothers (data not shown).

Teratogenic Effects of Hyperglycemia Are Developmental Stage-Specific

In the course of repeating the above described experiment, several times we noted that not all the conceptuses cultured in high-glucose conditions exhibited yolk sac vasculopathy. This apparent discrepancy can be explained by the fact that the conceptuses of a single mother are not all in the same developmental stage.³⁶ In our studies we found that a typical CD1 strain mother at 7.5 days p.c. was carrying a litter of 12 to 14 conceptuses, with 50% being in the primitive streak stages, 38% being in the neural plate stages, and 12% being in the headfold stages (Table 1). The incidence of yolk sac vasculopathy after culture in hyperglycemic conditions was 100% in primitive streak and neural fold stage embryos but only 9% in headfold stage embryos (Table 1). Upon separating harvested conceptuses into either primitive streak/neural fold stages and headfold stages we were able to elicit 100% yolk sac vasculopathy in the primitive streak/neural fold stage conceptuses, but no vasculopathy was noted in the headfold stage conceptuses.

In addition to the vasculopathy (arrest at the primary capillary plexus stage) observed in the yolk sacs of conceptuses cultured in hyperglycemic conditions, we also noted profound abnormalities in the embryos when high glucose exposure started at the primitive streak and neural fold stages of development (see Figure 8). These significant major embryonic abnormalities included open neural tube, failure of development of umbilical vessels from the allantois, cardiac abnormalities, and failure of proper axis formation (see Figures 8, A and B, and 9, B and D). In contrast, headfold stage 7.5 day p.c. conceptuses cultured in the same hyperglycemic conditions

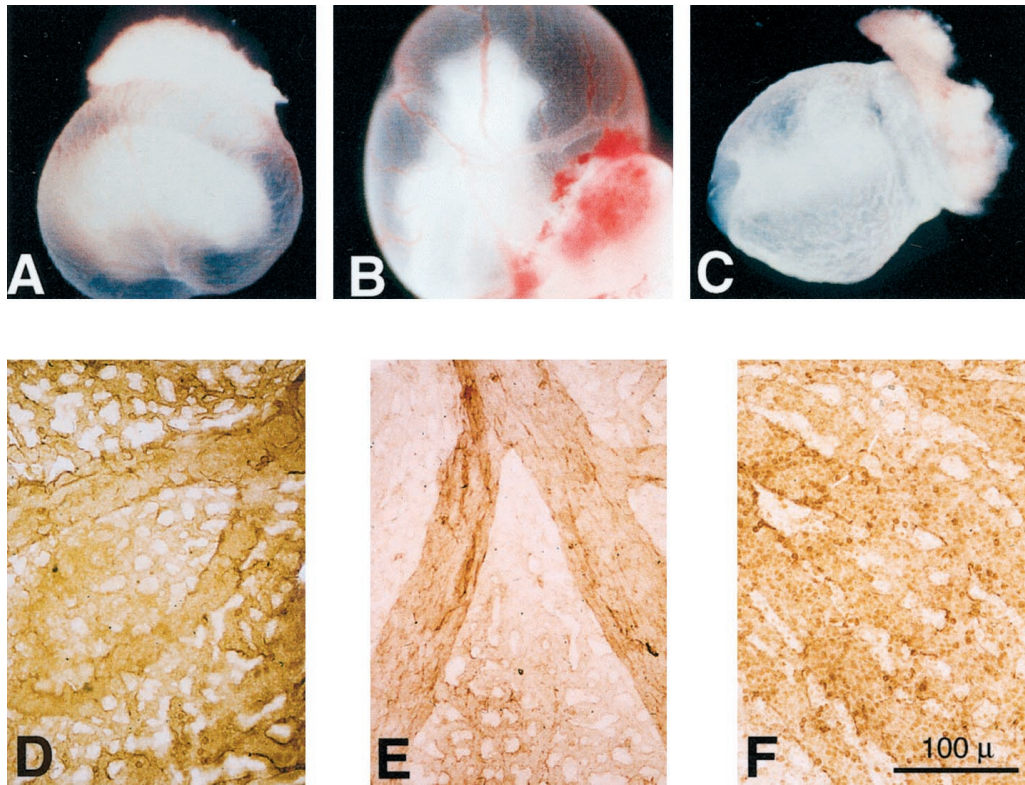


Figure 4. Morphological analyses of the developing yolk sac vasculature at day 9.5 p.c. in conceptuses harvested from normoglycemic mothers (A and D) and mothers made hyperglycemic by prior streptozotocin treatment (B and E and C and F). **A:** Representative 9.5 day p.c. normal conceptus harvested from a normoglycemic mother illustrating the normal delicate arborization of the yolk sac vasculature. **B:** Representative 9.5 day p.c. unaffected conceptus harvested from a hyperglycemic mother illustrating the normal delicate arborization of the yolk sac vasculature. **C:** Representative 9.5 day p.c. affected conceptus harvested from a hyperglycemic mother illustrating the arrest of yolk sac vasculo- and angiogenesis at the primary capillary plexus stage, illustrated by ectatic vascular channels with no apparent arborization. **D:** Low-power *en face* representative micrograph of the yolk sac vasculature observed in a normal conceptus harvested at day 9.5 p.c. from a control, normoglycemic mother. The yolk sac was labeled with anti-PECAM-1. Note the arborizing network of vessels composed of branching vessels of decreasing diameters as they branch from the larger vessels. **E:** Low-power *en face* representative micrograph of the yolk sac vasculature observed in an unaffected conceptus harvested at day 9.5 p.c. from a streptozotocin-treated hyperglycemic mother. The yolk sac was labeled with anti-PECAM-1. Note the arborizing network of branching vessels composed of branching vessels of decreasing diameters as they branch from the larger vessels. **F:** Low-power *en face* representative micrograph of the yolk sac vasculature observed in an affected conceptus harvested at day 9.5 p.c. from a streptozotocin-treated hyperglycemic mother. The yolk sac was labeled with anti-PECAM-1. Note the network of branching channels composed of ectatic vessel segments with occasional smaller branches having larger diameters than the terminal branching vessels observed in D. Scale bar, 100 μ m. Experiments were performed at least five times with separate litters.

exhibited less dramatic developmental abnormalities. Culture of conceptuses in sera containing exogenous α -L-glucose or D-mannitol resulted in no detectable abnormalities above control levels (Table 1).

Additionally, when primitive streak and neural plate stage conceptuses were exposed to 20 mmol/L D-glucose for varying time periods during culture, an incubation period of only 3 hours at the beginning of the 48-hour culture period was sufficient to induce the same vasculopathy/embryopathy as those conceptuses cultured for 48 hours in the continual presence of 20 mmol/L D-glucose (data not shown).

Conceptuses from Diabetic Mice Exhibit Vasculopathy Similar to That Observed in Conceptuses Cultured in Hyperglycemic Conditions

To confirm that the vasculopathy observed in conceptuses cultured in α -D-glucose-supplemented hyperglycemic media was a result of the hyperglycemic state, an *in*

vivo diabetic animal model was used. Of the 62 females injected with streptozotocin, 48 became diabetic. Female mice made diabetic by streptozotocin (serum glucose levels were 20 to 25 mmol/L) were kept normoglycemic with daily insulin treatment until successful mating. Of the 48 diabetic females, 25 became pregnant. Upon insulin withdrawal, hyperglycemia returned (serum glucose levels of 20 to 25 mmol/L), and the conceptuses were harvested at day 9.5 p.c. Litters from diabetic mothers were smaller compared with control mothers (8 to 9 *versus* 12 to 14), and the developing embryos were smaller than their normal counterparts. The uteri of diabetic mothers showed signs of resorption of implanted conceptuses. Of the 218 conceptuses harvested at day 9.5 p.c., 84 conceptuses (40%) exhibited vasculopathy and embryopathy whereas 124 (60%) appeared normal. Examination of the yolk sac vasculature of affected conceptuses of diabetic mothers (Figure 4C) compared with the yolk sac vasculature of unaffected conceptuses (Figure 4B) or conceptuses of control mothers (Figure 4A) revealed an apparent arrest at the primary capillary plexus stage, a lack of arborization, and ectasia of the capillary bed

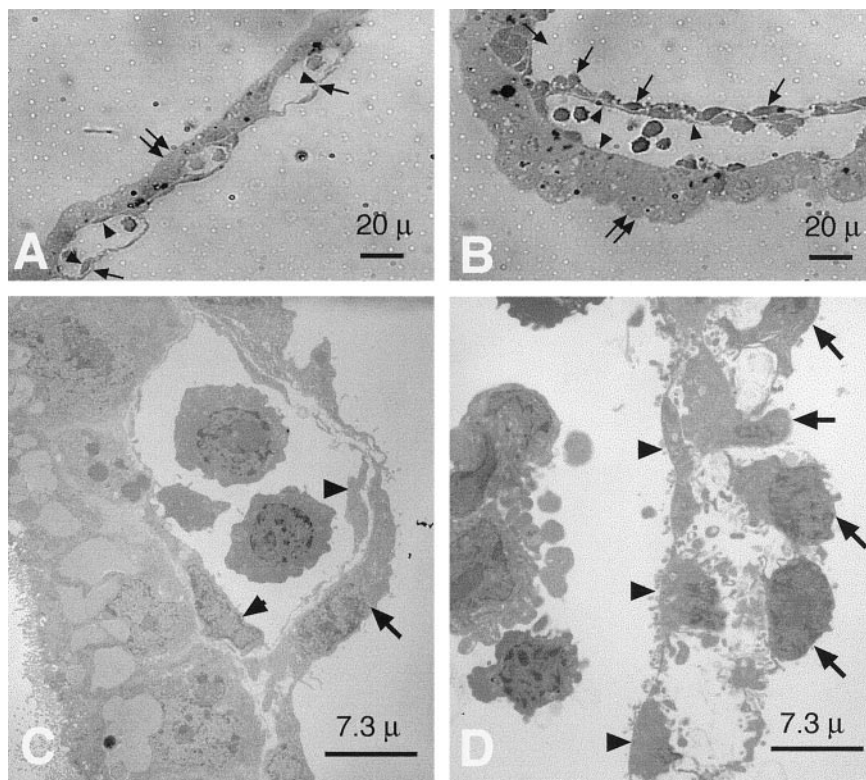


Figure 5. Light (A and B) and electron microscopic (C and D) analyses of the developing yolk sac vasculature at day 9.5 p.c. harvested from conceptuses of control (A and C) and streptozotocin-treated diabetic mothers (B and D). **A:** High-power representative light micrograph of the terminal yolk sac vasculature capillaries observed in a conceptus harvested at day 9.5 p.c. from a normoglycemic mother. Note the vessel lined by flattened endothelial cells (arrowheads) containing blood cells in the lumen, bordered by the endodermal cells on one aspect (double arrows) and flattened, elongated mesenchymal cells (pericytes) on the other aspect (arrows) in close contact with the abluminal surfaces of the endothelium. Scale bar, 20 μm . **B:** High-power representative light micrograph of the terminal yolk sac vasculature capillaries observed in a conceptus harvested at day 9.5 p.c. from a streptozotocin-treated diabetic mother. Note the vessel lined by flattened endothelial cells (arrowheads), bordered by endodermal cells on one aspect (double arrows) and plump, rounded mesenchymal cells (pericytes) on the other aspect (arrows) in loose contact with the abluminal surfaces of the endothelium. Several blood cells are present in the lumen. Scale bar, 20 μm . **C:** Representative transmission electron micrograph of the terminal yolk sac vasculature capillaries observed in a conceptus harvested at day 9.5 p.c. from a normoglycemic mother. Note the vessel lined by flattened endothelial cells (arrowheads) bordering the lumen and the flattened, elongated mesenchymal cells (pericytes) in close contact with the abluminal surfaces of the endothelium (arrows). Scale bar, 7.3 μm . **D:** Representative transmission electron micrograph of the terminal yolk sac vasculature capillaries observed in a conceptus harvested at day 9.5 p.c. from a streptozotocin-treated diabetic mother. Note the vessel lined by endothelial cells (arrowheads) bordering the lumen and the plump, rounded, mesenchymal cells (pericytes) in loose contact with the abluminal surfaces of the endothelium. Scale bar, 7.3 μm . Experiments were performed at least five times with separate litters.

similar to that observed in conceptuses cultured in 20 mmol/L αD -glucose (compare Figures 1B and 4C).

Further analysis of these yolk sacs revealed morphologies similar to those described in Figure 1. Namely, yolk sacs of affected embryos displayed ectatic capillary plexi without apparent arborization (Figure 4F) compared with the normal arborization noted in the yolk sacs of both control and unaffected conceptuses (Figure 4, D and E). Light and transmission electron microscopic analyses of these yolk sacs also revealed morphologies similar to those described in Figure 2. Cross sections of yolk sac capillaries from control conceptuses revealed small-diameter vessels lined by flattened, elongated endothelial cells containing occasional circulating blood cells and tightly invested by elongated, flattened mesenchymal and mesodermal cells (Figure 5, A C). In contrast, cross sections of yolk sac capillaries from affected conceptuses of streptozotocin-treated diabetic mothers revealed larger-diameter, ectatic capillaries filled with blood cells, demarcated by plump endothelial cells and loosely invested with plump, rounded mesenchymal and mesodermal cells (Figure 5, B and D). Conceptuses cultured with

media containing added L-glucose or D-mannitol were observed to develop normally, with no detectable abnormalities (see Table 1).

The 60% of the conceptuses from the diabetic mothers that developed normally (as assessed by gross morphological criteria) were smaller in size than control embryos, but no abnormalities were present in yolk sacs or embryos (data not shown).

Tyrosine Phosphorylation of PECAM-1 Is Modulated by the D-Glucose Levels of the Pregnant Mother

Biochemical analyses of PECAM-1 expression and tyrosine phosphorylation state of control conceptuses and unaffected and affected conceptuses from diabetic mothers revealed no appreciable differences in PECAM-1 expression but an increase in PECAM-1 tyrosine phosphorylation in PECAM-1 immunoprecipitated from affected conceptuses of diabetic mothers exhibiting vasculopathy (Figure 6, compare lanes 1 and 2 with lane

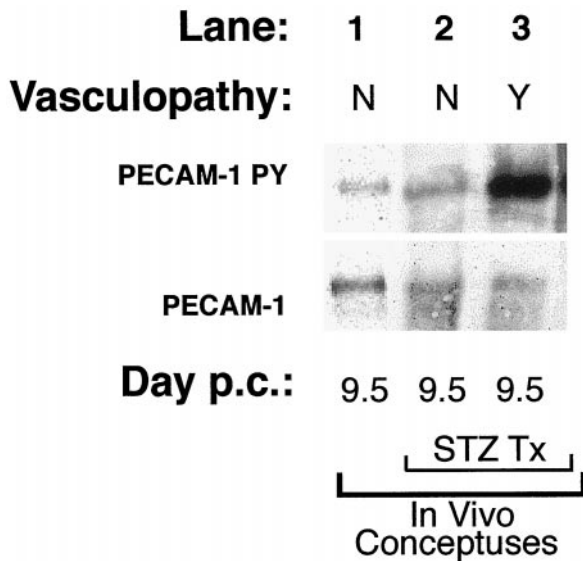


Figure 6. Representative immunoprecipitation/Western blot analyses of PECAM-1 expression and tyrosine phosphorylation of normal (lane 1), unaffected (lane 2), and affected (lane 3) day 9.5 p.c. conceptuses isolated from normoglycemic (lane 1) and hyperglycemic (lanes 2 and 3) mothers. Note the similar expression levels of PECAM-1 obtained when the conceptus lysates were immunoprecipitated with anti-PECAM-1 and then blotted using anti-PECAM-1 (lower panel). Stripping and reprobing these blots with anti-phosphotyrosine revealed relatively higher tyrosine phosphorylation of PECAM-1 at day 9.5 p.c. in the hyperglycemic lysates (lane 3, upper panel) derived from conceptuses exhibiting yolk sac vasculopathy (Y) compared with the low tyrosine phosphorylation levels noted in the lysates derived from unaffected conceptuses from hyperglycemic and normoglycemic mothers exhibiting normal yolk sac vascular development (N) (lanes 1 and 2). See Figure 7, lanes 5 and 6 (3.65 versus 1.00 when quantitated, normalized to PECAM-1 expression and compared). Experiments were performed five times with separate litters, all yielding similar results.

3; see Figure 7, 0.90 ± 0.17 versus 3.65 ± 1.17 , $n = 3$, $P < 0.05$). This increase in PECAM-1 tyrosine phosphorylation is similar to that observed in conceptuses cultured in hyperglycemic conditions (compare Figures 3 and 6).

The Effects of Hyperglycemia on PECAM-1 Tyrosine Phosphorylation State and on Embryonic Vasculature Are Similar in Both in Vitro and in Vivo Models

Comparison of the effects of hyperglycemia on *in vitro* and *in vivo* yolk sac PECAM-1 tyrosine phosphorylation states revealed similar increases (Figure 7, 2.53 ± 0.99 *in vitro* versus 3.65 ± 1.17 *in vivo*, $n = 3$, $P = 0.16$) in both instances.

In addition to the similarities in the yolk sac vasculopathy (compare Figures 1 and 2 with 4 and 5) and PECAM-1 tyrosine phosphorylation states (compare Figure 3 with Figures 6 and 7), examination of the embryos exposed to hyperglycemic culture conditions and embryos harvested from streptozotocin-treated diabetic mothers also revealed similar abnormalities. These include failure of neural tube closure (Figure 8, B and D, solid arrows), failure of proper umbilical vessel formation due to abnormal allantois development (Figure 8, B and D, dashed arrows), and abnormal axis rotation (Figure 8, B and D). Additionally, in affected embryos, visceral organs and

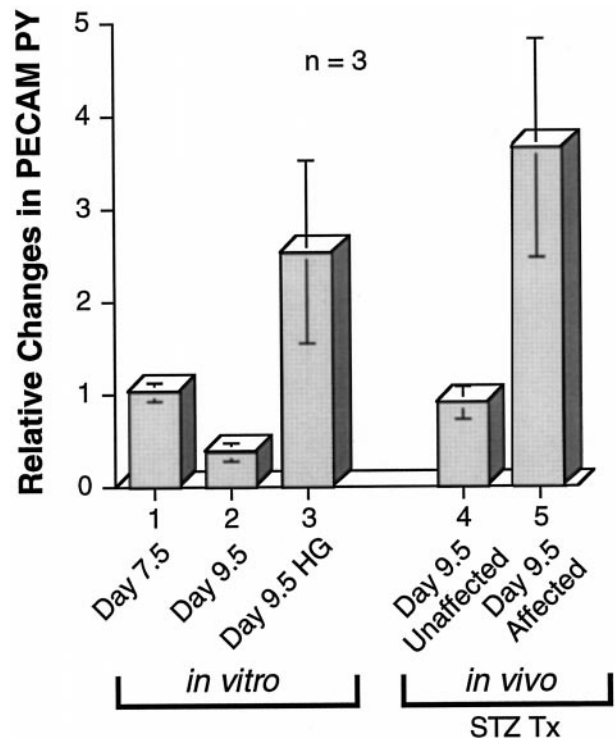


Figure 7. Quantitation of observed changes in day 9.5 p.c. yolk sac PECAM-1 tyrosine phosphorylation states after 48 hours of *in vitro* and *in vivo* hyperglycemia (see Figures 3 and 6 for details). Conceptuses (harvested at day 7.5 p.c.) were put in culture in the absence (day 9.5) or presence (day 9.5 HG) of 20 mmol/L α -D-glucose for 48 hours. Note the significant decrease in yolk sac PECAM-1 tyrosine phosphorylation after 48 hours in normoglycemic culture (day 9.5, compare lanes 1 and 2) compared with the significant increase in PECAM-1 tyrosine phosphorylation after 48 hours in hyperglycemic culture (day 9.5 HG, compare lanes 1 and 2 with 3). Yolk sacs of unaffected day 9.5 p.c. conceptuses harvested from streptozotocin-treated (STZ Tx) diabetic mothers exhibited significantly lower levels of yolk sac PECAM-1 tyrosine phosphorylation compared with the increased yolk sac PECAM-1 tyrosine phosphorylation of abnormal day 9.5 p.c. conceptuses exhibiting vasculopathy (day 9.5 affected, compare lanes 4 and 5). $n = 3$; bars are standard deviations.

neural tubes were pale and showed abnormal vascularization (data not shown).

Microscopic analysis of the embryonic hearts revealed failure of endocardial cushion formation (Figure 9). Specifically, the development of the epicardium, myocardium, and endocardium appeared normal in all conditions studied. Further examination of the hearts revealed a failure of endocardial cushion development in the cultured embryos made hyperglycemic with 20 mmol/L D-glucose, (Figure 9, B and D) and in the affected embryos harvested from hyperglycemic mothers (Figure 9, F and H), manifested by a failure of endocardial cells to dissociate from the endocardial lining and migrate into the underlying cardiac jelly.^{41,42}

Discussion

Yolk sac and embryonic vasculogenesis and the establishment of the vitelline circulation are crucial for initial organogenesis and further embryonic growth and development. Subsequent development of the placental circulation and further embryonic angiogenesis are critical for

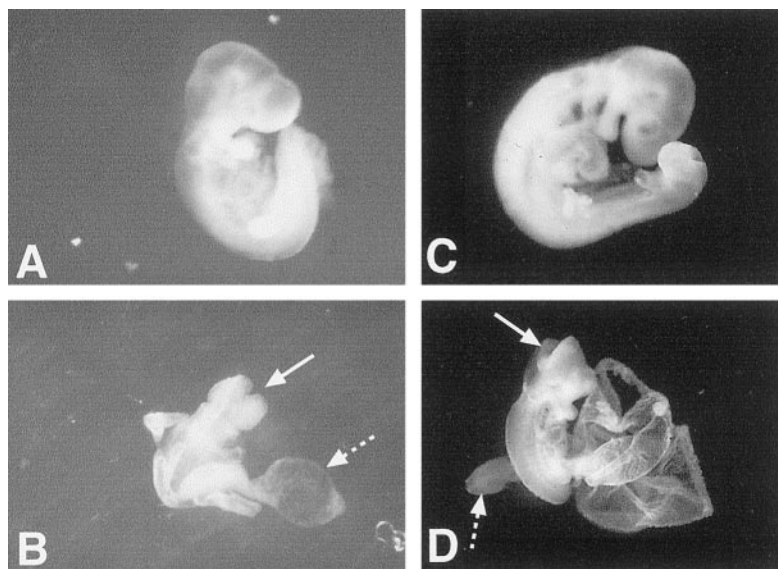


Figure 8. Whole-mount micrographs of 7.5 day p.c. embryos cultured in normoglycemic (A) and hyperglycemic (B) conditions for 48 hours and 9.5 day p.c. embryos harvested from control, normoglycemic mothers (C) and streptozotocin-treated diabetic mothers (D). A: Note the normal development and organogenesis of the representative embryo cultured in normoglycemic conditions for 48 hours. B: Representative embryo harvested at 7.5 days p.c. at the primitive streak and neural fold stages and cultured for 48 hours in sera containing 20 mmol/L α -D-glucose exhibited dramatic maldevelopment. Illustrated here are open neural tube (arrow), maldevelopment of the allantois (dashed arrow), and failure of normal axis rotation. C: Representative embryo at 9.5 days p.c. harvested from a control, normoglycemic mother. Note the normal development and organogenesis. D: Representative embryo at 9.5 day p.c. harvested from a streptozotocin treated diabetic mother. Illustrated here are open neural tube (arrow), maldevelopment of the allantois (dashed arrow), and failure of normal axis rotation.

the normal development of the organ systems and survival of the embryo/fetus. Disruption of mesoderm development in several mice exhibiting targeted disruptions, including knock-outs of fibronectin, α 5 and α 4 integrins, VCAM-1, tissue factor, and vinculin, results in profound yolk sac vascular maldevelopment and embryonic lethality.^{17,20–23,43} Recently, an embryonic lethal knock out of Ephrin B2 was also noted to result in yolk sac vasculopathy, characterized by a block to remodeling at the primary capillary plexus stage and failure of appropriate mesodermal (pericyte) investiture of the developing yolk sac vasculature as well as selective embryonic vasculopathy.¹⁷ Additionally, VEGFR1, VEGFR2, VEGF, TIE-1, and TIE-2 knock-out mouse studies revealed blocks in the vasculo- and angiogenesis pathways, leading to failures of endothelial cell differentiation, vessel formation, pericytic investiture, and vascular integrity, resulting in either embryonic or perinatal lethality.^{10–16,25–27} These studies illustrate the complex, incompletely understood interactions among different families of soluble, cell-surface, and solid-phase (extracellular matrix) ligands and their receptors in the processes of embryonic vasculo- and angiogenesis.

We have previously determined that PECAM-1 is a modulator of *in vitro* and *in vivo* angiogenesis and endothelial cell-cell interactions and migration *in vitro* and that PECAM-1 tyrosine phosphorylation regulates endothelial cell behavior.^{29,30,32} Thus, we reasoned that the dynamic tyrosine phosphorylation of endothelial PECAM-1 may be affected in the embryonic vasculopathy induced by hyperglycemia in culture and by experimental diabetes. Maternal diabetes mellitus is associated with embryonic lethality and congenital abnormalities, including a wide range of cardiovascular abnormalities.^{1–8} Using whole

embryo cultures, we have previously demonstrated that the observed embryonic abnormalities were always accompanied by abnormalities in the visceral endodermal layer of the yolk sac and abnormal yolk sac vascularization.⁷ More recently, we reported that during the development of the vitelline vasculature PECAM-1 is highly expressed, and the state of PECAM-1 tyrosine phosphorylation correlated with the development of the yolk sac vasculature (ie, the development of blood islands and vessels from hemangioblasts).³²

In the present study we have demonstrated that conceptuses cultured in hyperglycemic medium as well as in conceptuses harvested from diabetic pregnant mice exhibit a similar arrest of yolk sac vasculo-angiogenesis at the primitive capillary plexus stage. This vasculopathy consists of the presence of ectatic vessels with a lack of development of proper arborization, similar to findings noted in embryonic lethal ephrin 2B, tissue factor, TGF- β 1, and TIE-2 homozygous null mice.^{17,27,43} Additionally, conceptuses cultured in hyperglycemic medium as well as harvested from diabetic pregnant mice exhibited an arrest of the normal PECAM-1 tyrosine dephosphorylation observed during vasculogenesis/angiogenesis.³² This inhibition of tyrosine dephosphorylation and its potential effects on SHP-2 binding and activity³¹ may be responsible for aberrant signaling, leading, in part, to the observed maldevelopment of the vasculature.

The lack of proper arborization results in the lack of development of normal branching patterns of arteries and veins and a lack of circulation within the vitelline system. Our data suggest that although the early aspects of new blood vessel formation (the process of vasculogenesis) is completed, the generation of blood vessels by sprouting and intussusception to form larger and

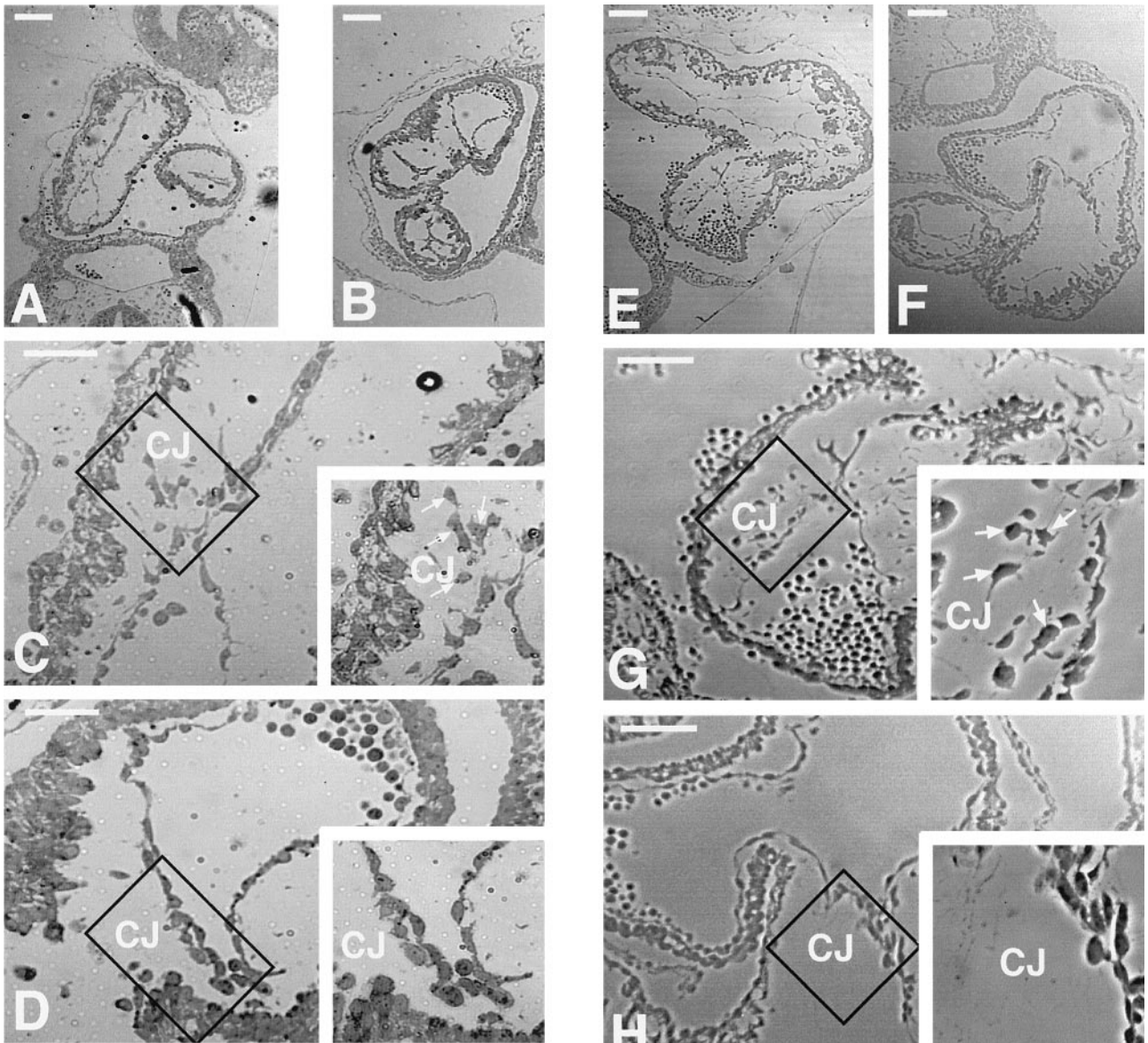


Figure 9. Light micrographs of 1- μ m sections of developing hearts from a representative cultured normoglycemic 9.5 day p.c. embryo culture (A and C), a representative cultured hyperglycemic 9.5 day p.c. embryo culture (B and D), a representative embryo at 9.5 days p.c. harvested from a control, normoglycemic mother, and a representative affected embryo at 9.5 days p.c. harvested from a hyperglycemic mother. Although the development of the epicardium, myocardium, and endocardium appears normal in all instances (A, B, E, and F), upon further examination of the hearts we noted a failure of endocardial cushion development in the embryos cultured in hyperglycemic media (20 mmol/L D-glucose, B and D) and in the affected embryos harvested from hyperglycemic mothers (F and H). Specifically, as illustrated in D and H, there is a failure of migration of endocardial cells overlying putative cushion areas into the cardiac jelly (CJ). Compare normal cushion development at this stage of development (C and C inset and G and G inset, which illustrate this migration (arrows)) to the arrest of cushion development (D and D inset and H and H inset, which illustrate a failure of migration of endocardial cells into the cardiac jelly (CJ)). Scale bars, 100 μ m. Experiments were performed five times with separate litters.

smaller vessels and eventually a functional adult circulatory system is interrupted after exposure to hyperglycemia. In addition, the embryopathy observed in the hyperglycemia-exposed conceptuses may also be the result, in part, of the maldevelopment of the developing vascular beds in different embryonic organs. As mentioned above, previous studies indicated that proper vascular maturation required interactions between endothelial cells, extracellular matrix, and other cells such as smooth muscle cells or pericytes.^{9,10,12,40,43} Our data also demonstrate a loss of intimate contacts between mesodermal cells (putative pericytes) and endothelial cells in yolk sacs exhib-

iting vasculopathy. This failure of development of endothelial cell-pericyte interactions is thought to be important in vessel stabilization and maturation.^{11,40,43} Whether the failure of PECAM-1 dephosphorylation and perturbation of SHP-2 binding and activity are also observed in these particular knock-out mice (angiopoietin-1, TIE-2, TGF- β 1, tissue factor, and ephrin 2B knock-outs) remains to be determined.

Our findings of a relatively short (3-hour) exposure time and a developmental-stage-specific susceptibility to hyperglycemic insult is consistent with a developmental-stage-dependent susceptibility. Our observations of con-

ceptuses of individual mothers exhibiting developmental stage variability is in agreement with the observations of Downs and Davies,³⁶ who noted developmental stage variability in the conceptuses harvested from individual mothers. Our studies of the conceptuses of individual mothers reveal that the yolk sac vasculature of conceptuses at earlier developmental stages (primitive streak and neural plate), when the yolk sac mesoderm is differentiating into hemangioblasts, is profoundly affected by hyperglycemic insult. In contrast, at later developmental stages (headfold), when the yolk sac hemangioblasts have formed blood islands, the yolk sac vasculature is spared and other embryonic vascular beds undergoing vasculo- and angiogenesis (brain and allantois) are affected. These findings suggest that only vascular beds undergoing active vasculo/angiogenesis are susceptible to the teratogenic effect of hyperglycemia. In addition to the arrest and failure of the development of the vitelline circulation, hyperglycemia induced major maldevelopment of several organ systems, manifested by persistence of open neural tubes, failure of proper axial rotation, malformation of the allantois, lack of development of umbilical vessels, arrested development of brain vasculature, and failure of endocardial cushion development. The apparent failure of endocardial cell migration (epithelial to mesenchymal transformation) necessary for successful endocardial cushion formation^{41,42} is consistent with a modulation of endothelial cell migration by PECAM-1. We have previously demonstrated that the tyrosine phosphorylation state of PECAM-1 determines, in part, endothelial cell migratory rates.^{30,34} Although we have not yet determined the tyrosine phosphorylation state of endocardial cells at this stage of development, this potential explanation is a reasonable one to investigate in the future.

These findings suggest that the teratogenic effects of high glucose on embryonic development is likely developmental stage specific and, in part, can be related to the interruption of the ongoing vasculo/angiogenesis of different organs. Based on these observations we conclude that the sensitive window period of hyperglycemic exposure that results in a deleterious effect on development is shorter than originally reported.²

The mechanism(s) involved in mediating the effects of hyperglycemia on yolk sac and embryonic vascular development are currently unknown. As only D-glucose and not L-glucose or D-mannitol elicits this effect, changes in osmolarity can be ruled out (Table 1).⁷ Possibilities that remain to be tested include 1) determining levels of glucose metabolites and assessing them as potential mediators of this embryopathy, 2) assessing dynamic tissue/organ-specific expression of particular glucose transporters during vasculo- and angiogenesis, and 3) assessing the levels and activities of tyrosine and serine/threonine kinases and phosphatases as modulators of PECAM-1 phosphorylation^{44,45} (N. Ilan, S. Mahooti, and J. A. Madri, submitted) and selected adapter and signaling molecules known to associate with PECAM-1, such as c-src and SHP-2.^{29-32,34} In previous studies, investigators have demonstrated glucose-induced changes in PECAM-1 serine/threonine phosphorylation⁴⁵; thus, it

would be useful to assess levels, phosphorylation states, and kinase activities of other known modulators of vasculogenesis/angiogenesis and mesenchymal cell recruitment, including VEGF, angiopoietin 1 and 2, the receptor tyrosine kinases VEGFR_{1,2}, Tie-1, and Tie-2 as well as ephrin B2 and ephB4, as targeted disruptions of several of these proteins exhibit similar abnormalities in the development of their yolk sac vasculature to those observed in this study.^{15-17,27} In addition, changes in blood flow could also have significant effects on vascular development and PECAM-1 tyrosine phosphorylation state. Circulation (blood flow) was found to be compromised in D-glucose-treated conceptuses and PECAM-1 tyrosine phosphorylation is known to be affected by changes in shear stress.⁴⁶

Thus, the *in vitro* model of hyperglycemic vasculopathy appears to mirror morphological and biochemical changes in vascular development noted in an *in vivo* model of maternal diabetes. In addition, it provides a controllable, manipulatable culture system to investigate a variety of pathological conditions associated with hyperglycemia and their underlying mechanisms. Coupled with the use of conceptuses harvested from heterozygous mice containing the lacZ indicator gene in frame with the initiation codon of genes of choice including TGF- β s, TGF- β Rs, VEGFRs, angiopoietin 1 and 2, Tie-1 and Tie-2, and ephrin B2 and eph-B4, this approach should provide needed insights into the roles of these molecules in both normal and abnormal vascular development.

References

1. Baker L, Piddington R: Diabetic embryopathy: a selective review of recent trends. *J Diabetes Comp* 1993, 7:404-412
2. Cockroft DL, Coppola PT: Teratogenic effects of excess glucose on head-fold rat embryos in culture. *Teratology* 1977, 16:141-146
3. Eriksson UJ, Hakan-Borg LA, Forsberg H, Styruud J: Diabetic embryopathy: studies with animal and in vitro models. *Diabetes* 1991, 40(Suppl 2):94-98
4. Ferencz C, Rubin JD, McCarter RJ, Clark EB: Maternal diabetes and cardiovascular malformations: predominance of double outlet right ventricle and truncus arteriosus. *Teratology* 1990, 41:319-326
5. Kitzmiller JL, Buchanan TA, Kjos S, Combs AC, Ratner RE: Pre-conception care of diabetes, congenital malformations, and spontaneous abortions. *Diabetes Care* 1996, 19:514-541
6. Pampfer S, Vanderheyden I, McCracken JE, Vesela J, De Hertogh R: Increased cell death in rat blastocysts exposed to maternal diabetes in utero and to high glucose or tumor necrosis factor-alpha in vitro. *Development* 1997, 124:4827-4836
7. Pinter E, Reece EA, Leranath CZ, Sanyal MK, Hobbins JC, Mahoney MJ, Naftolin F: Yolk sac failure in embryopathy due to hyperglycemia: ultrastructural analysis of yolk sac differentiation associated with embryopathy in rat conceptuses under hyperglycemic conditions. *Teratology* 1986, 33:73-84
8. Reece EA, Hornko CJ, Wu YK: Multifactorial basis of the syndrome of diabetic embryopathy. *Teratology* 1996, 54:171-182
9. Folkman J, D'Amore PA: Blood vessel formation. What is its molecular basis? *Cell* 1996, 87:1153-1155
10. Hanahan D: Signaling vascular morphogenesis and maintenance. *Science* 1997, 277:48-50
11. Lindahl P, Johansson BR, Leveen P, Betsholtz C: Pericyte loss and microaneurism formation in PDGF-beta deficient mice. *Science* 1997, 277:242-245
12. Risau W: Mechanisms of angiogenesis. *Nature* 1997, 386:671-674
13. Shalaby F, Rossant J, Yamaguchi TP, Gertsenstein G, Wu X-F, Brellt

- man ML, Schuh AC: Failure of blood island formation and vasculogenesis in Flk-1-deficient mice. *Nature* 1995, 376:62–66
14. Shalaby F, Ho J, Stanford WL, Fischer KL, Schuh AC, Schwartz L, Bernstein A, Rossant J: A requirement for Flk1 in primitive and definitive hematopoiesis and vasculogenesis. *Cell* 1997, 89:981–990
 15. Suri C, Jones PF, Patan S, Bartunkova S, Maisonpierre PC, Davis S, Sato TN, Yancopoulos GD: Requisite role of angiopoietin-1, a ligand for the TIE2 receptor, during embryonic angiogenesis. *Cell* 1996, 87:1171–1180
 16. Vikkula M, Boon LM, Carraway KL III, Calvert JT, Diamonti AJ, Goumnerov B, Pasyk KA, Marchuk DA, Warman ML, Cantley LC, Mulliken JB, Olsen BR: Vascular dysmorphogenesis caused by an activating mutation in the receptor tyrosine kinase TIE2. *Cell* 1996, 87:1181–1190
 17. Wang HU, Chen ZF, Anderson DJ: Molecular distinction and angiogenic interaction between embryonic arteries and veins revealed by ephrin-B2 and its receptor Eph-B4. *Cell* 1998, 93:741–753
 18. Xu W, Baribault H, Adamson ED: Vinculin knockout results in heart and brain defects during embryonic development. *Development* 1998, 125:327–337
 19. Yancopoulos GD, Klagsbrun M, Folkman J: Vasculogenesis, angiogenesis, and growth factors. Ephrins enter the fray at the border. *Cell* 1998, 93:661–664
 20. Yang JT, Rayburn H, Hynes RO: Embryonic mesodermal defects in alpha5 integrin-deficient mice. *Development* 1993, 85:149–158
 21. Yang JT, Rayburn H, Hynes RO: Cell adhesion events mediated by alpha4 integrins are essential in placental and cardiac development. *Development* 1995, 121:549–560
 22. George EL, Georges EN, Patel-King RS, Rayburn H, Hynes RO: Defects in mesodermal migration and vascular development in fibronectin-deficient mice. *Development* 1993, 119:1079–1091
 23. Kwee L, Baldwin HS, Shen HM, Stewart CL, Buck C, Buck CA, Labow MA: Defective development of the embryonic and extraembryonic circulatory systems in vascular cell adhesion molecule (VCAM-1) deficient mice. *Development* 1995, 121:489–503
 24. Carmeliet P, Ferreira V, Breier G, Pollefeyt S, Kieckens L, Gertsenstein M, Harpal K, Eberhardt C, Declercq C, Pawling J, Moons L, Collen D, Risau W, Nagy A: Abnormal blood vessel development and lethality in embryos lacking a single VEGF allele. *Nature* 1996, 380:435–439
 25. Maisonpierre PC, Suri C, Jones PF, Bartunkova S, Wiegand SJ, Radziejewski C, Compton D, McClain J, Aldrich TH, Papadopoulos N, Daly TJ, Davis S, Sato TN, Yancopoulos GD: Angiopoietin-2 a natural antagonist for Tie2 that disrupts in vivo angiogenesis. *Science* 1997, 277:55–60
 26. Fong G-H, Rossant J, Gertsenstein M, Brechtman ML: Role of the Flt-1 receptor tyrosine kinase in regulating the assembly of vascular endothelium. *Nature* 1995, 376:66–70
 27. Sato TN, Tozawa Y, Deutsch U, Wolburg-Buchholz K, Fujiwara Y, Gendron-Maguire M, Gridley T, Wolburg H, Risau W, Qin Y: Distinct roles of the receptor tyrosine kinases Tie-1 and Tie-2 in blood vessel formation. *Nature* 1995, 376:70–74
 28. Baldwin SH, Shen HM, Yan HC, DeLisser HM, Chung A, Mickanin C, Trask T, Kirschbaum NE, Newman PJ, Albelda SM, Buck CA: Platelet endothelial cell adhesion molecule-1 (PECAM-1/CD31): alternatively spliced, functionally distinct isoforms expressed during mammalian cardiovascular development. *Development* 1994, 120:2539–2553
 29. Lu TT, Barreuther M, Davis S, Madri JA: Platelet endothelial cell adhesion molecule-1 is phosphorylatable by c-src, binds src-src homology 2 domain, and exhibits immunoreceptor tyrosine-based activation motif-like properties. *J Biol Chem* 1997, 272:14442–14446
 30. Lu TT, Yan LG, Madri JA: Integrin engagement mediates tyrosine dephosphorylation of platelet-endothelial cell adhesion molecule 1. *Proc Natl Acad Sci USA* 1996, 93:11808–11813
 31. Newman PJ: The biology of PECAM-1. *J Clin Invest* 1997, 99:3–8
 32. Pinter E, Barreuther M, Lu TT, Imhof BA, Madri JA: Platelet-endothelial cell adhesion molecule-1 (PECAM-1/CD31) tyrosine phosphorylation state changes during vasculogenesis in the murine conceptus. *Am J Pathol* 1997, 150:1523–1530
 33. Schimmenti LA, Yan HC, Madri JA, Albelda SM: Platelet endothelial cell adhesion molecule-1, PECAM-1, modulates cell migration. *J Cell Physiol* 1992, 153:417–428
 34. Kim CS, Wang T, Madri JA: Platelet endothelial cell adhesion molecule-1 expression modulates endothelial cell migration in vitro. *Lab Invest* 1998, 78:583–590
 35. Piali L, Hammel P, Uherek C, Bachmann F, Gislis RH, Dunon D, Imhof BA: CD31/PECAM-1 is a ligand for alpha_v beta₃ integrin involved in adhesion of leukocytes to endothelium. *J Cell Biol* 1995, 130:451–460
 36. Downs KM, Davies T: Staging of gastrulating mouse embryos by morphological landmarks in the dissecting microscope. *Development* 1993, 118:1255–1266
 37. Cockroft DL: Dissection and culture of postimplantation embryos. *Postimplantation Mammalian Embryos: A Practical Approach*. Edited by Copp AJ, Cockroft DL. Oxford, Oxford University Press 1990, pp 15–40
 38. Ment LR, Stewart WB, Ardito TA, Madri JA: Germinal matrix microvascular maturation correlates inversely with the risk period for neonatal intraventricular hemorrhage. *Dev Brain Res* 1995, 84:142–149
 39. Kaufman MH (editor): *The Atlas of Mouse Development*. London, Academic Press, 1990, pp 5–85
 40. Hirschi KK, D'Amore PA: Pericytes in the microvasculature. *Cardiovas Res* 1996, 32:687–698
 41. Markwald RR, Fitzharris TP, Adams Smith, WN: Structural analysis of endocardial cytodifferentiation. *Dev Biol* 1975, 42:160–180
 42. Markwald RR, Fitzharris TP, Manasek FJ: Structural development of endocardial cushions. *Am J Anat* 1977, 148:85–120
 43. Carmeliet P, Mackman N, Moons L, Luther T, Gressens P, Van Vlaenderen I, Demunck H, Kasper M, Breier G, Evard P, Muller M, Risau W, Edgington T, Collen D: Role of tissue factor in embryonic vessel development. *Nature* 1996, 383:73–75
 44. Esser S, Lampugnani GL, Corada M, Dejana E, Risau W: Vascular endothelial growth factor induces VE-cadherin tyrosine phosphorylation in endothelial cells. *Cell Sci* 1998, 111:1853–1865
 45. Rattan V, Shen Y, Sultana C, Kumar D, Kalra VK: Glucose-induced transmigration of monocytes is linked to phosphorylation of PECAM-1 in cultured endothelial cells. *Am J Physiol* 1996, 271:E711–E717
 46. Osawa M, Masuda M, Harada N, Bruno R, Lopes RB, Fujiwara K: Tyrosine phosphorylation of platelet endothelial cell adhesion molecule-1 (PECAM-1, CD31) in mechanically stimulated vascular endothelial cells. *Eur J Cell Biol* 1997, 72:229–237